Available online at www.sciencedirect.com
SCIENCE DIRECT
Developmental Biology 290 (2006) 359 – 372
DEVELOPMENTAL BIOLOGY
www.elsevier.com/locate/ydbio

# Foxd3 mediates zebrafish *myf5* expression during early somitogenesis

Hung-Chieh Lee, Hsing-Yen Huang, Cheng-Yung Lin, Yau-Hung Chen [1], Huai-Jen Tsai *

*Institute of Molecular and Cellular Biology, National Taiwan University, No. 1, Section 4, Roosevelt Road, Taipei 106, Taiwan*

Received for publication 27 May 2005, revised 17 November 2005, accepted 22 November 2005
Available online 4 January 2006

**Abstract**

Myf5, one of the basic helix–loop–helix transcription factors, controls muscle differentiation and is expressed in somites during early embryogenesis. However, the transcription factors bound to the *cis*-elements of *myf5* are poorly understood. In this study, we used the yeast one-hybrid assay and found that Forkhead box d3 (Foxd3) interacted specifically with the −82/−62 cassette, a key element directing somite-specific expression of *myf5*. The dual-luciferase assay revealed that the expression of Foxd3 potently transactivated the *myf5* promoter. Knocking down *foxd3* with morpholino oligonucleotide (MO) resulted in a dramatic down-regulation of *myf5* in somites and adaxial cells but not in the presomitic mesoderm. On the other hand, *myod* expression remained unchanged in *foxd3* morphants. Foxd3 mediation of *myf5* expression is stage-dependent, maintaining *myf5* expression in the somites and adaxial cells during the 7- to 18-somite stage. Furthermore, in the *pax3* morphant, the expression of *foxd3* was down-regulated greatly and the expression of *myf5* was similar to that of the *foxd3* morphant. Co-injection of *foxd3* mRNA and *pax3*-MO1 greatly restored the expression of *myf5* in the somites and adaxial cells, suggesting that *pax3* induces *foxd3* expression, which then induces the expression of *myf5*. This report is the first study to show that Foxd3, a well-known regulator in neural crest development, is also involved in *myf5* regulation.


*Keywords:* *myf5*; *foxd3*; *pax3*; Zebrafish; Myogenesis

## Introduction

In vertebrates, the specification of muscle progenitor cells in the somites depends on inductive signals emanating from adjacent tissues, such as the neural tube, the notochord, and the dorsal and lateral ectoderm. In response to inducers, muscle precursor cells (myoblasts) start expressing several transcriptional activators that control the expression of muscle structural genes. A family of muscle regulatory factors (MRFs) with a basic DNA binding motif and a basic helix–loop–helix dimerization domain has been identified in mammals, birds, frogs, fish, insects, and nematodes (Michelson et al., 1990; Hopwood et al., 1991; Buonanno et al., 1992; Saitoh et al., 1993; Krause et al., 1994; Chen et al., 2000, 2001). Proteins in this family include Myod (Davis et al., 1987), Myogenin (Braun et al., 1989a; Edmondson and Olson, 1989; Wright et al., 1989), Myf5 (Braun et al., 1989b), and MRF4/herculin/Myf6 (Rhodes and Konieczny, 1989; Braun et al., 1990; Miner and Wold, 1990).

In mice, Myf5 is activated at different anatomical sites in the embryo under the control of distinct, *cis*-acting regulatory elements (Hadchouel et al., 2000; Summerbell et al., 2000; Carvajal et al., 2001). An enhancer, 6.6 kb upstream, is required for *myf5* expression in the epaxial domain (Gustafsson et al., 2002). A 270-bp core enhancer, about 57 kb upstream, directs *myf5* expression in limbs and maintains *myf5* expression in somites (Buchberger et al., 2003). Another enhancer directs *myf5* expression in cervical somites and restricts *myf5* transcription in the myotome. In *Xenopus*, two negative regulatory elements have been identified in the *Xmyf5* promoter, which controls *Xmyf5* expression. An interferon regulatory factor-like DNA binding element down-regulates *Xmyf5* expression in differentiating myocytes (Mei et al., 2001), and a distal TCF-3 binding site restricts *Xmyf5* expression in the midline mesoderm by means of Wnt/β-catenin signals (Yang et al., 2002). A T-box binding site mediates dorsal activation of *Xmyf5* transcription and is involved in the regulation of muscle development (Lin et al., 2003). In zebrafish *myf*5, the upstream sequence −82 to −1

* Corresponding author. Fax: +886 2 2363 8483.
*E-mail address:* hjtsai@ntu.edu.tw (H.-J. Tsai).
[1] Present address: Graduate Institute of Life Sciences, Tamkang University, Taipei, Taiwan.

0012-1606/$ - see front matter © 2005 Elsevier Inc. All rights reserved.
doi:10.1016/j.ydbio.2005.11.032

(−82/−1) directs reporter gene expression specifically in the somites but the −62/−1 segment cannot (Chen et al., 2001). Recently, Chen et al. (2003) demonstrated that the −82/−62 regulatory cassette in zebrafish *myf5* is a *cis*-element that is able to direct somite-specific expression and repress nonspecific expression during early embryogenesis. Although promoter analysis and identification of *cis*-regulatory elements have been carried out with mouse, *Xenopus*, and zebrafish *myf5*, the *trans*-acting factors that actually bind to *cis*-acting elements in *myf5* remain unknown.

Somite patterning is under the control of a variety of signals provided by the dorsal neural tube, notochord, floor plate, surface ectoderm, and lateral plate mesoderm (Münsterberg et al., 1995; Marcelle et al., 1997; Pourquié et al., 1996; Hirsinger et al., 1997; Yamaguchi, 1997; Currie and Ingham, 1998; Tajbakhsh et al., 1998; Reshef et al., 1998). Several transcription factors and signaling modulators, such as bone morphogenetic protein 4 (BMP4; Cossu et al., 1996), Noggin (Hirsinger et al., 1997), Wnt (Ikeya and Takada, 1998; Tajbakhsh et al., 1998; Borycki et al., 1999), Sonic Hedgehog (Shh; Coutelle et al., 2001), Gli (Gustafsson et al., 2002), and Pax3 (Marcelle et al., 1995; Maroto et al., 1997; Tajbakhsh et al., 1997), play important roles in mediating the response of signals from surrounding tissues to induce expression of MRFs. The regulatory network of mouse *myf5* has been elucidated (Cossu and Borello, 1999; Buckingham, 2001; Roth et al., 2003; Tajbakhsh, 2003), and it is proposed that *pax3* regulates mouse *myf5* expression in an indirect manner (Maroto et al., 1997; Tajbakhsh et al., 1997; Roth et al., 2003). However, the detailed molecular interaction among factors in the regulatory network during the time of commitment to modulate *myf5* expression has yet to be revealed.

In this study, using a yeast one-hybrid assay, we determined that Foxd3 interacted specifically with the −82/−62 regulatory element of zebrafish *myf5*. Foxd3 also plays an important role in maintaining *myf5* expression in the somites and adaxial cells. This Foxd3 mediation of *myf5* is stage-dependent. Furthermore, we demonstrate that the expression of *foxd3* in the *pax3* morphant was down-regulated greatly and that the expression of *myf5* was similar to that of the *foxd3* morphant. Injection of *foxd3* mRNA rescued the defects caused by *pax3* morpholino oligonucleotide (MO), suggesting that *pax3* induces *foxd3* expression, which then induces the expression of *myf5*. This article is the first study to demonstrate that Foxd3 mediates *myf5* expression and is involved in myogenesis during zebrafish embryogenesis.

## Materials and methods

### *Yeast one-hybrid screening*

Yeast one-hybrid screening was performed according to the protocol of the manufacturer (Clontech). The bait plasmids pHISi-6× (−82/−62) and pLacZi-6× (−82/−62) were constructed using synthetic DNA oligomers containing six repeats of the *myf5* −82/−62 cassette. Four plasmids were used in the selection procedure as negative controls. They included p53HIS, which contains the consensus p53 binding site; pGAD424, which contains only the GAL4 activation domain; and pHISi-m4m5 and pLacZi-m4m5, which contain four repeats of the *myf5* −82/−62 cassette in which the −70/−62 sequence was mutated to GAAGTTAAC (m4m5; Chen et al., 2003). The cDNA was inserted into a plasmid, pGADT7-Rec, by homologous recombination in yeast. Transformed plasmids were recovered with a yeast plasmid isolation kit (Clontech). The plasmids isolated from each clone were transformed into *Escherichia coli* DH5α cells for amplification.

### *Fish embryos*

Zebrafish (AB strain) were maintained at 28.5°C under a 14-h light/10-h dark photoperiod. After fertilization, eggs were collected and cultured in an aquarium. The number of embryonic cleavages was counted, and somite formation was observed under a fluorescent stereomicroscope MZ FLIII (Leica).

### *Knockdown microinjection of zebrafish embryos*

MOs were obtained from Gene Tools. The sequences of MOs were designed as follows: *foxd3*-MO1, TGCTGCTGGAGCAACCCAAGGTAAG, antisense nucleotides 160 to 184 of zebrafish *foxd3* cDNA (GenBank accession no. AF052249); *foxd3*-MO2, CACTGGTGCCTCCAGACAGGGTCAT, antisense nucleotides 197 to 221 of zebrafish *foxd3* cDNA; *foxd3*-MO-sense, ATGACCCTGTCTGGAGGCACCAGTG, sense nucleotides 197 to 221 of zebrafish *foxd3* cDNA; *pax3*-MO1, GCTAATGCGGTCATATCTCCTCTGC, antisense nucleotides 266 to 290 of zebrafish *pax3* cDNA (GenBank accession no. NM131277); *pax3*-MO2, ACGAAAAAAGGATGCACGAAGCACT, antisense nucleotides 241 to 265 of zebrafish *pax3* cDNA; *myf5*-MO, TACGTCCATGATTGGTTTGGTGTTG, antisense nucleotides 28 to 52 of zebrafish *myf5* cDNA (GenBank accession no. NM131576). All oligonucleotides were prepared at a stock concentration of 1 mM and diluted to the desired concentration for microinjection into each embryo.

### *Electrophoretic mobility shift assay*

The −82/−62 cassette, the mutated sequence of −82/−62 (sequence at −70/−62 was mutated to GAAGTTAAC; m4m5) and a nonspecific sequence (Non-30fr) were used as oligonucleotide probes for the binding assay (Chen et al., 2003). All probes were labeled with γ-[$^{32}$P]ATP (3,000 μCi/ml) using T4 polynucleotide kinase (NEB). Probes, recombinant Foxd3 protein (50 or 500 ng), and 1 μg of poly(dIdC) were added to the reaction buffer (10 mM Tris at pH 7.5, 50 mM NaCl, 0.5 mM ethylenediaminetetraacetic acid pH 8.0, 0.5 mM dithiothreitol, 5% glycerol) and incubated at 30°C for 30 min. Unlabeled −82/−62 cassette, Non-30fr, and m4m5 were used for competitive inhibition. After reacting, all products were analyzed by 6% acrylamide gel electrophoresis (79:1 acrylamide:bisacrylamide). After transferring the bands to a 3M filter and drying the gel, X-ray film was exposed to the sample for 2 days.

### *Cloning zebrafish Foxd3 cDNA and plasmid constructions*

Full-length cDNA coding for zebrafish *foxd3* was obtained by polymerase chain reaction (PCR) from a cDNA library of 14–18 h postfertilization (hpf) zebrafish embryos using the 5′-primer CTCGAGATGACCCTGTCTGGAGGCACC and the 3′-primer CTCGAGTCATTGAGAAGGCCATT in which an *Xho*I site was included. The PCR products were first ligated into pGEMT-easy vector (Promega), then digested by *Xho*I, and subcloned into a pET-15b vector (Novagen). The coding region of zebrafish *foxd3* was amplified by PCR using the 5′-primer GGTACCATGACCCTGTCTGGAGGCACC, in which a *Kpn*I site was included, and the 3′-primer TCATTGAGAAGGCCATTTCGATACCG. The PCR products were subcloned into the pGEMT-easy vector (Promega), digested by *Kpn*I and *Not*I, then cloned into the pCMVm vector, which contains the CMV promoter and enhancer (Chen et al., 2003). Plasmids pZMYP-2937E and pZMYP-6212E, to which green fluorescent protein was fused with the upstream 3 and 6 kb of zebrafish *myf5*, respectively, were described previously (Chen et al., 2001). Plasmid pRL-ZMYP3.0, containing an upstream 2.9 kb of zebrafish *myf5* that was recovered from an *Age*I–*Pst*I-cut pZMYP-2937E, was subcloned into the *Nhe*I–*Pst*I-cut phRL-Null vector (Promega) in which the *Nhe*I was blunted. Plasmid pRL-ZMYP6.0, containing the upstream 6.2 kb of *myf5* that was recovered from an *Age*I–*Pst*I-cut

pZMYP-6212E, was subcloned into the phRL-Null vector by using the same strategy.

### *Preparation of recombinant proteins in vitro*

*E. coli* BL21 (DE3)/pLysS containing zebrafish *foxd3* cDNA was cultured to produce recombinant Foxd3. Following induction, *E. coli* was treated with 0.5 mM isopropyl-1-thio-β-D-galacto-pyranoside for 4 h at 37°C. After the cells were lysed, recombinant Foxd3 was purified with a Ni-NTA spin column (Qiagen).

### *Cell culture*

Monkey kidney COS-1 cells were cultured in Dulbecco's modified Eagle's medium (DMEM, Biowest) containing 10% fetal bovine serum (Biowest), which was heat-inactivated by incubating for 30 min at 56°C, supplemented with 1× penicillin/streptomycin/glutamine (Biowest), and then incubated at 37°C in an atmosphere of 5% $CO_2$ and 95% air. Fresh culture medium was provided every 2 or 3 days, and the cells were subcultured before reaching 70% confluency. The embryonal carcinoma cell line P19 was cultured in alpha minimum essential medium (Gibco), 7.5% bovine calf serum (Biowest), 2.5% fetal bovine serum, and 1× penicillin/streptomycin/glutamine. Medium was renewed at least every 48 h and subcultured every 2 or 3 days.

### *Dual-luciferase assay*

About $1 \times 10^5$ cells were seeded onto each well of six-well plates 24 h prior to transfection. Cells were transfected by the lipofectamine method (Invitrogen) according to the manufacturer's instruction. Transfection mixtures normally contained 6 μl of lipofectamine and 1 to 2 μg of plasmid constructs of firefly luciferase and *Renilla* luciferase (RL). After a 48-h transfection, cells were harvested for luciferase assay by using the Dual-Luciferase Reporter Assay System (Promega). Luciferase activity was measured from three separated experiments in a Luminoskan Ascent (Thermo Labsystems).

### *RNA in situ hybridization*

Whole-mount in situ hybridization of whole embryos was performed by using digoxigenin (DIG) -labeled riboprobes of *myf5*, *foxd3, myod*, *myogenin,* and *α-actin*. We followed the procedures as described by Chen et al. (2001), except that phosphate-buffered saline with 0.1% Tween 20, 2 mg/ml bovine serum albumin, 5% sheep serum, and 1% dimethyl sulfoxide were used in the blocking solution. To determine the co-localization of *myf5* and *foxd3* transcripts, double in situ hybridizations were performed following the scheme of Jowett (2001), except that *foxd3* was labeled with fluorescein-UTP (Roche) and *myf5* was labeled with DIG-UTP (Roche).

### *mRNA injection for the rescue experiment*

Capped mRNAs of *foxd3*, *myf5*, and red fluorescent protein (RFP) were synthesized according to the protocol of the manufacturer (Epicentre). The resulting mRNA was diluted to 11 or 22 ng/μl for *foxd3* mRNA, 130 or 260 ng/μl for *myf5* mRNA, and 44 ng/μl for RFP mRNA with distilled water, and 2.3 nl of each was injected into 1-cell stage embryos. In the rescue experiments, embryos were observed at 13- to 16-somite stage in terms of morphological defects and the expression patterns of target genes by using whole mount in situ hybridization.

## Results

### *Foxd3 is the cognate protein bound to the myf5 −82/−62 cassette*

Yeast one-hybrid screening was used to identify the factor bound to the −82/−62 cassette of zebrafish *myf5*. Six copies of the −82/−62 cassette were inserted in the region upstream of the *Saccharomyces cerevisiae* selection marker YM4271. A cDNA library constructed from mRNA of 15–18 hpf embryos was screened, and $8.5 \times 10^3$ clones were grown on minimal medium. About 162 colonies that not only were able to grow on the selective medium but that also were *lac*Z-positive were isolated. Then, their insert DNA fragments were cloned and sequenced. After these cDNA sequences were identified from the gene bank using the BLAST procedure, we selected 83 putative colonies containing the full-length cDNA and back-transformed them into yeasts. Finally, there were 17 colonies containing cDNA fragments that were able to interact specifically with the −82/−62 bait. One of these colonies containing *foxd3* cDNA was chosen for further study because this cDNA insert was somite-positive after in situ hybridization. The binding specificity of Foxd3 and −82/−62 cassette was evaluated with two assays. First, recombinant yeasts, containing Foxd3 fused to the activation domain Gal4, grew in the selective medium only when they contained the wild-type *myf5* −82/−62 cassette. Recombinant yeasts harboring the mutated sequence within −82/−62 did not grow (Fig. 1A). Second, β-galactosidase activity was detected in yeasts containing Foxd3 fused with the activation domain when the *myf5* −82/−62 cassette was upstream of *lac*Z. However, β-galactosidase activity was not detectable in yeasts containing mutated sequences of the *myf5* −82/−62 cassette (Fig. 1B).

### *Electrophoretic mobility shift assay demonstrates that recombinant Foxd3 binds to the −82/−62 cassette*

Electrophoretic mobility shift assay (EMSA) was used to determine whether the *myf5* −82/−62 cassette is able to bind Foxd3 in vitro. Recombinant Foxd3 produced by *E. coli* interacted specifically with the −82/−62 probe, producing the shifted band shown on the gel (Fig. 2). In addition, the shifted band of DNA–protein complex was lost completely when excess amounts of cold −82/−62 oligonucleotides were added. But, neither the nonspecific DNA competitor (Non30fr; Fig. 2, lane 7) nor the mutated −82/−62 competitor (m4m5; Fig. 2, lane 6) interfered by forming a specific complex between recombinant Foxd3 and the −82/−62 probe. Thus, the interaction between Foxd3 and the *myf5* −82/−62 cassette is specific.

### *Transactivation of the myf5 promoter by Foxd3*

To test the functional consequences of Foxd3 interactions with the *myf5* −82/−62 cassette, we performed transient transfection assays with a luciferase reporter gene under the control of the zebrafish *myf5* promoter in the COS-1 and P19 cell lines. The upstream 3-kb or 6-kb region of zebrafish *myf5* was cloned to the phRL-Null vector. Results showed that the luciferase activity in COS-1 cells in the presence of recombinant Foxd3 was 2.4-fold (pRL-ZMYP3.0) or 2.6-fold (pRL-ZMYP6.0) greater than that of the untreated group after 48-hr transfection ($n = 4$, $P < 0.05$; Fig. 3). This case was also the finding when we used the P19 cells: the luciferase

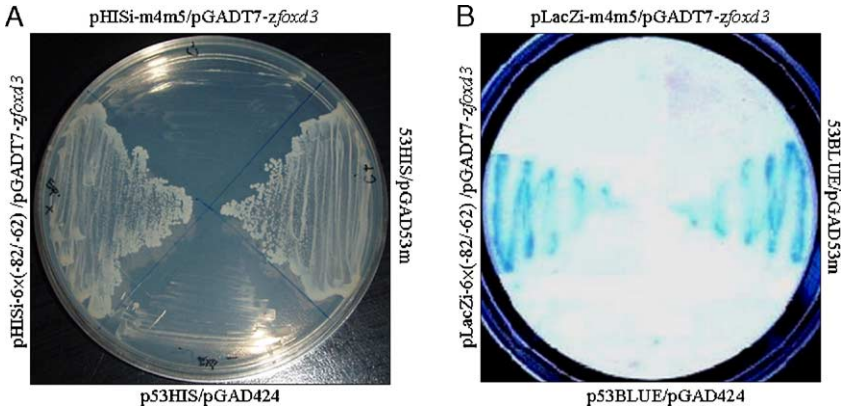


Fig. 1. The yeast one-hybrid system was used to identify Foxd3 bound to the *myf5* −82/−62 cassette. (A) The yeast one-hybrid assay of clones transfected with the plasmids indicated the following: pHISi-6× (−82/−62), which contains six repeats of −82/−62; pGADT7-*zfoxd3*, which contains *foxd3* with the GAL4 activation domain; pHISi-m4m5, which contains the mutated −82/−62 cassette; p53HIS/pGAD53m, the positive control; p53HIS/pGAD424, the negative control. Yeasts that harbored plasmids containing wild-type −82/−62 grew under growth-inhibiting conditions (histidine and leucine were absent, 60 mM of 3-amino-1,2,4-triazole was present) when Foxd3 fused to the activation domain was expressed. Yeasts containing plasmids with mutated −82/−62 did not grow. (B) The colony-lift filter method was used to perform β-galactosidase assays. Yeasts were transformed, as indicated, with each of the following plasmids: pLacZi-6× (−82/−62), the bait plasmid that contains six repeats of −82/−62 and carries the *lacZ* reporter gene; pLacZi-m4m5, which contains four repeats of the mutated −82/−62 sequence; p53BLUE/pGAD53m, the positive control; p53BLUE/pGAD424, the negative control. Positive β-galactosidase activity, shown in blue, was detected only when the *foxd3* activation domain fusion was expressed in yeasts containing wild-type −82/−62. No activity was detected in yeasts with mutated −82/−62.

activity was increased 3.65-fold (pRL-ZMYP3.0) or 4.16-fold (pRL-ZMYP6.0) by the presence of Foxd3 ($n = 4$, $P < 0.05$; Fig. 3). Thus, we conclude that the interaction between Foxd3 and the *myf5* promoter resulted in transactivation of gene expression.

### *Expression patterns of myf5 and foxd3 were colocalized*

The pattern of *foxd3* expression in zebrafish embryos varied with developmental stage. During the 4- to 6-somite stage, *foxd3* was transcribed in the floor plate, presumptive neural crest cells, and tail bud (Fig. 4A). During the 7- to 9-somite stage, *foxd3* expression was first detected in the somites (Fig. 4B, arrowhead) and the signals also appeared in the posterior premigratory crests and tail bud. During the 11- to 16-somite stage, *foxd3* was expressed strongly in the somites and the signals in the neural crest cells were down-regulated prior to neural crest migration (Figs. 4C, D). However, faint signals in the lateral head and in the loose cluster of *foxd3*-positive cells in the posterior head increased incrementally with the formation of each pair of somites (Figs. 4C, D, arrow). In embryos with 16–28 somites, *foxd3* expression in the somites was high but was down-regulated rapidly in the somites after the 28-somite stage (data not shown). Use of double in situ hybridization to detect both the *myf5* and the *foxd3* transcripts at the 11- to 13-somite stage revealed that the expression domains of *myf5* and *foxd3* coincided greatly in somites and adaxial cells (Figs. 4E, F), indicating that the expression patterns of *foxd3* and *myf5* were colocalized.

### *In the foxd3 morphant, morphological defects were dose-dependent*

To determine whether Foxd3 affects *myf5* expression in vivo, we used two different MOs: one complementary to 25 bp of the 5′-untranslated region of *foxd3* mRNA (*foxd3*-MO1) and the other complementary to 25 bp after AUG of *foxd3* mRNA (*foxd3*-MO2). Embryos that received two types of *foxd3*-MOs displayed similar defective phenotypes, whereas embryos that received only the control MO (*foxd3*-MO-sense) developed normally, even when we injected it at a concentration as high as 8 ng/embryo (Table 1). When 4–10 ng of *foxd3*-MOs were injected, morphants with 12–14 somites displayed defects in the head and the tail bud (Figs. 5A, B). Although the frequency of segmentation defects did not differ in wild-type and *foxd3*-MO1-injected embryos, the somites of *foxd3* morphants became broader than the somites of wild-type embryos (Figs. 5C, D). Most abnormalities were mild and included a raised tail, a reduced head, and wider somites with an irregular boundary. Minor abnormalities led to serious defects that retarded development. It is interesting to note that the defects caused by injecting two *foxd3*-MOs were dose-dependent and synergistic (Table 1). To confirm whether the *foxd3*-MO-induced defects were specific, we co-injected synthetic *foxd3* mRNA and *foxd3*-MO1. The *foxd3*-MO1 was used because it was complementary to a sequence of the 5′-untranslated region, i.e., it blocked the endogenous *foxd3* mRNA but not the microinjected *foxd3* mRNA. Synthetic *foxd3* mRNA (25–50 pg) largely rescued the morphological defects induced by *foxd3*-MO1 (Table 1), suggesting that the *foxd*3-MO-induced defects were specific.

### *Effects of foxd3 on myf5 expression are stage-dependent*

To determine whether the states of differentiation of the somites were affected in *foxd3* morphants, we assayed the expression of a number of genes that are normally expressed in somites and other tissues. *myf5* expression domains in the presomitic mesoderm (PSM) of *foxd3* morphants and wild-type embryos were the same, but no signals were detected in

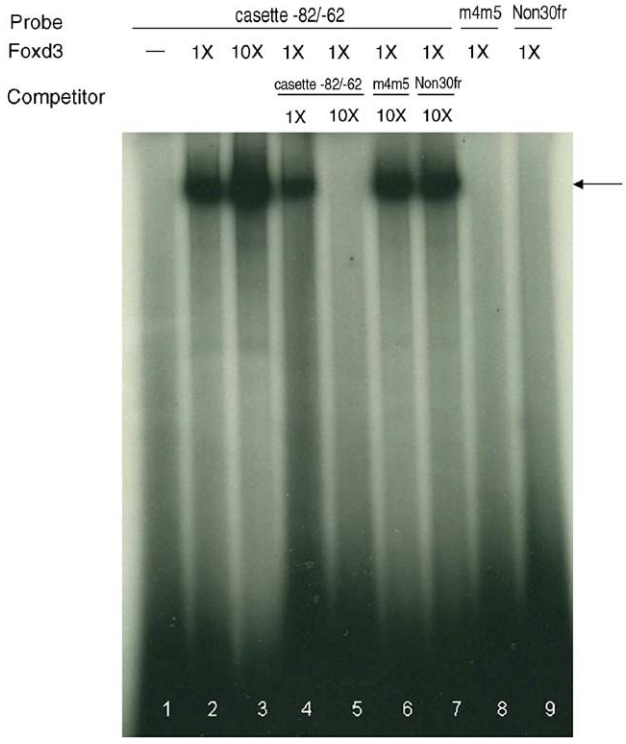


Fig. 2. Binding between purified recombinant Foxd3 and $^{32}$P-radiolabeled oligonucleotide probes was studied with the electrophoretic mobility shift assay. The arrow indicates the shifted band formed by double-stranded oligonucleotide and recombinant Foxd3. Three probes were used: cassette −82/−62, mutated −82/−62 (m4m5, in which the −70/−62 sequence was mutated), and a nonspecific DNA sequence (Non-30fr). Radiolabeled cassette −82/−62, without added nuclear extracts, was the negative control (lane 1). The shifted bands were abolished completely when excess amount of unlabeled −82/−62 oligonucleotide was added (lanes 4 and 5). Recombinant Foxd3 did not bind to m4m5 (lane 8) or Non30fr (lane 9). In addition, m4m5 and Non30fr competitors did not compete for binding with Foxd3 and cassette −82/−62 (lanes 6 and 7).

the somites and adaxial cells during the 8- to 10-somite stage (Figs. 6A, G). During the 11- to 13-somite stage, *myf5* gene expression in morphants was inactivated in the somites and adaxial cells (located on the lateral portions of somites 1–9) but signals in the PSM were not lost (Figs. 6B, H). Meanwhile, *myf5* expression decreased greatly in the somites and the adaxial cells during the 14- to 16-somite stage, but *myf5* transcripts were expressed normally in the PSM (Figs. 6C, I). In *foxd3* morphants, *myf5* was expressed normally in the PSM: these embryos did not lose *myf5* expression patterns in somites 0 and −1 (Figs. 6G–J, arrowheads). However, the *myf5* signals greatly decreased in the newly formed somites and in the completely formed somites, indicating that *foxd3* functions to maintain *myf5* gene expression in the somites but not in the PSM during somitogenesis.

After the 17- to 19-somite stage, endogenous *myf5* expression was down-regulated and differences in *myf5* expression between wild-type embryos and *foxd3* morphants became negligible (Figs. 6D, J). This down-regulated expression pattern persisted for wild-type embryos and *foxd3* morphants after the 20- to 24-somite stage (Figs. 6E, F vs. Figs. 6K, L). However, at these stages, the expression level of *foxd3* in the somites was still strong. This evidence clearly demonstrated that the regulation of *myf5* through *foxd3* was stage-dependent. Moreover, we also found an unexpected ectopic expression of *myf5* in the tail bud in *foxd3* morphants with raised tails (Fig. 6H, arrow), suggesting that Foxd3 may play other roles in the tail bud.

### *Foxd3 modulates expression of myf5 but not myod*

We compared the expression of two genes involved in somitogenesis in *foxd3* morphants and wild-type embryos. In *foxd3* morphants, both *myogenin* (which is downstream of *myf5*) and *α-actin* (the structural protein in somites) clearly were down-regulated in the somites but were expressed normally in adaxial cells (Figs. 7C, D, G, H). However, *myod* expression in the somites and adaxial cells remained unchanged (Figs. 7B, F). Furthermore, we noticed that 10 somites were positive for *myod* staining in wild-type embryos, whereas 6 were positive in the *foxd3*-MO1-injected embryos. This difference may be due to development delay in MO-treated embryos. Thus, we suggest that Foxd3 specifically regulated the expression of *myf5* but not *myod*.

### *foxd3 knockdown morphant can be rescued by injecting myf5 mRNA*

To determine whether the *foxd3* morphant phenotype could be rescued by *myf5*, we co-injected *foxd3*-MO1 and synthetic *myf5* mRNA. A series of different concentrations of *myf5* mRNA was injected together with 8 ng of *foxd3*-MO1 into

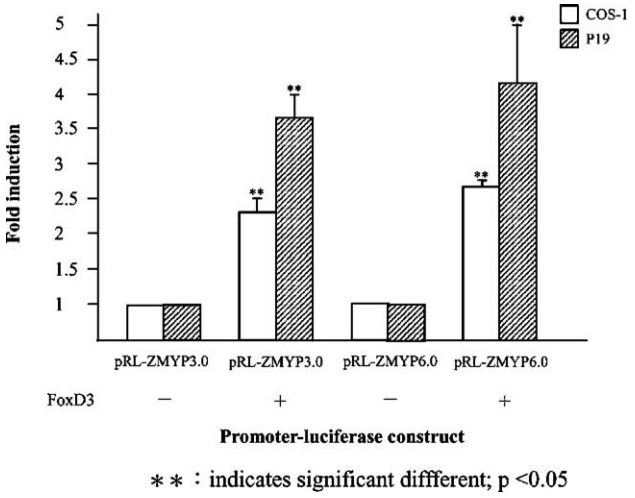


Fig. 3. Transactivation of the *myf5* promoter by Foxd3. Cultured cell lines COS-1 and P19 were used to study whether Foxd3 transactivates the expression of zebrafish *myf5*. In the dual-luciferase assay, luciferase activity was represented as the fold increase compared to the absence of recombinant Foxd3. In COS-1 cells, the luciferase activity increased 2.4-fold (pRL-ZMYP3.0) or 2.6-fold (pRL-ZMYP6.0) when the recombinant Foxd3 was present. In the P19 cell line, the luciferase activity increased 3.65-fold (pRL-ZMYP3.0) or 4.16-fold (pRL-ZMYP6.0) when Foxd3 was present. All transfections and luciferase assays were performed independently at least three times. Data are means ± S.D. Asterisks indicate a mean is significantly different ($P < 0.05$).

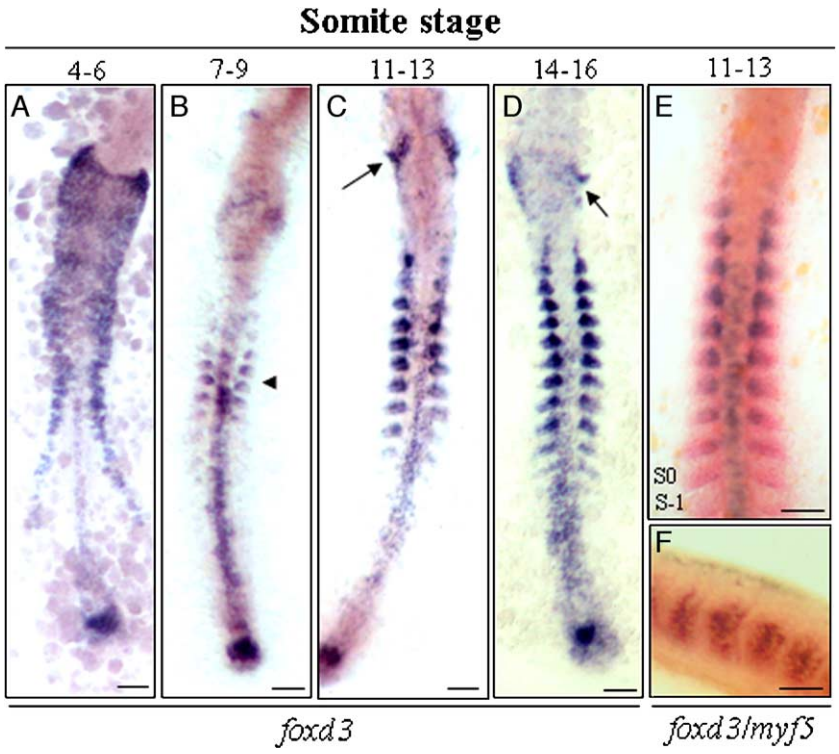


Fig. 4. Temporal and spatial expression of *foxd3* in zebrafish embryos at different somite stages. (A) At the 4- to 6-somite stage, *foxd3* was transcribed in the floor plate, presumptive neural crest cells, and tail bud. (B) At the 7- to 9-somite stage, *foxd3* transcripts were first detected in the somites (arrowhead) and the signals were weak in migrating neural crest cells. In addition to the somitic mesoderm, *foxd3* mRNA also was found in the tail bud and posterior premigratory crest. (C, D) At the 11- to 16-somite stage, *foxd3* transcription increased incrementally after each pair of somites was formed. *foxd3* transcripts in the lateral head were down-regulated, but *foxd3* expression was strong in the somites and cranial ganglia posterior to the otic vesicle (arrow). (E, F) In the 11- to 13-somite stage of wild-type embryos, double in situ hybridization using red-labeled *myf5* and blue-labeled *foxd3* probes was used to show that expressions of these genes were colocalized in the posterior part of the somites. Scale bars: 100 μm.

eggs. The expression of *myogenin* and *α-actin* was rescued partially by injecting *myf5* mRNA compared to the expression in embryos that were injected with *foxd3*-MO1 alone (Table 2; Fig. 7G vs. J; Fig. 7H vs. K). Co-injection of *myf5* mRNA effectively rescued the expression of *myogenin* (from 7% to 51% of defects) and *α-actin* (from 32% to 53% of defects) at the concentration range of 300–600 pg (Table 2). Moreover, embryos that were injected with *myf5*-MO showed reduced expression of *myogenin* but not of *myod* (Fig. 7I). The expression pattern of *myogenin* in *foxd3* morphants and in *myf5* morphants was similar. Taken together, our data suggest that *myf5* mRNA effectively rescues the *foxd3* morphant phenotype and that the *foxd3*-MO1 used in this study specifically inhibits *myf5* expression.

### *Molecular control of pax3, foxd3, and myf5*

To define further the molecular network among *pax3*, *foxd3,* and *myf5* during zebrafish myogenesis, we injected *pax3*-MOs into embryos to repress *pax3* expression. Like the strategy of using *foxd3*-MOs, two *pax3*-MOs were designed: *pax3*-MO1 and *pax3*-MO2. Embryos that received *pax3*-MO1 displayed severe convergence/extension phenotypes. The defects caused by these two MOs were similar, dose-dependent, and synergistic (Table 1). We found that *foxd3* expression was down-regulated significantly (Fig. 8D vs. E). Meanwhile, *myf5* expression was restricted in the PSM and weak in somites 0 and −1 and in the adaxial cells on the sides of somites 0 and −1 (Figs. 8A, B). The patterns of *myf5* expression were similar in morphants derived from embryos treated with *foxd3*-MO1 and *pax3*-MO-1 (Figs. 7E, 8B). However, in *pax3* morphants, *myod* clearly was down-regulated in the somites but was expressed normally in adaxial cells (Figs. 8F, G). Furthermore, we found that, when 25 pg of *foxd3* mRNA and 6 ng *of pax3*-MO1 were co-injected, the expression of *myf5* was greatly restored in the somites (Fig. 8C), but it did not rescue *myod* expression in the somites (Fig. 8H). Based on these findings, we conclude that (1) *foxd3* specifically regulates expression of *myf5* but not *myod,* (2) *pax3* acts as an upstream regulator of *foxd3,* and (3) down-regulation of *myf5* in *pax3* morphants occurs because *foxd3* is not expressed.

## Discussion

The winged helix transcription factor *forkhead* gene was first described in *Drosophila* (Weigel et al., 1989). Rodent *HNF3* transcription factor is very similar (Weigel and Jäckle, 1990; Lai et al., 1990, 1991). Forkhead domains have been reported in organisms ranging from yeasts to humans (Lai et al., 1993). Based on conserved residues at distinct positions in the DNA binding domain, more than 10 different classes of *forkhead* genes have been described. Some classes have been

Table 1
Morphological phenotypes of zebrafish embryos derived from fertilized eggs injected with different materials

| Injected materials | Concentration | Number of embryos surviving among number of injected eggs | Wild-type phenotype | Number of embryos with abnormal phenotypes | |
|---|---|---|---|---|---|
| | | | | Mild defects | Severe defects |
| *foxd3*-MO1 | 4 ng | 169/224 (75.4%) | 127 (75.1%) | 42 (21.6%) | 0 (0%) |
| *foxd3*-MO1 | 8 ng | 133/155 (85.8%) | 56 (42.1%) | 65 (48.9%) | 12 (9.0%) |
| *foxd3*-MO1 | 10 ng | 179/247 (72.5%) | 27 (15.1%) | 107 (59.8%) | 45 (25.1%) |
| *foxd3*-MO2 | 4 ng | 132/154 (85.7%) | 96 (72.7%) | 30 (22.6%) | 6 (4.5%) |
| *foxd3*-MO2 | 8 ng | 124/159 (78.0%) | 12 (9.7%) | 92 (74.2%) | 20 (16.1%) |
| *foxd3*-MO1 + *foxd3*-MO2 | 2 + 2 ng | 75/89 (84.3%) | 22 (29.3%) | 40 (53.3%) | 13 (17.3%) |
| *foxd3*-MO-sense | 4 ng | 124/127 (97.6%) | 124 (100%) | 0 (0%) | 0 (0%) |
| *foxd3*-MO-sense | 8 ng | 83/84 (98.8%) | 83 (100%) | 0 (0%) | 0 (0%) |
| *myf5*-MO | 4 ng | 72/73 (98.6%) | 2 (2.8%) | 68 (94.4%) | 2 (2.8%) |
| *pax3*-MO1 | 6 ng | 92/124 (74.2%) | 24 (26.1%) | 53 (57.6%) | 15 (16.3%) |
| *pax3*-MO2 | 6 ng | 77/95 (81.1%) | 26 (33.8%) | 49 (63.6%) | 2 (2.6%) |
| *pax3*-MO1 + *pax3*-MO2 | 3 ng + 3 ng | 81/104 (77.9%) | 19 (23.5%) | 59 (72.8%) | 3 (3.7%) |
| *dsRed* mRNA | 100 pg | 71/79 (89.9%) | 71 (100%) | 0 (0%) | 0 (0%) |
| *foxd3* mRNA + *foxd3*-MO1 | 25 pg + 8 ng | 136/151 (90.1%) | 82 (60.3%) | 50 (36.8%) | 4 (2.9%) |
| *foxd3* mRNA + *foxd3*-MO1 | 50 pg + 8 ng | 128/144 (88.9%) | 104 (81.3%) | 24 (18.7%) | 0 (0%) |
| *myf5* mRNA + *foxd3*-MO1 | 300 pg + 8 ng | 192/257 (74.7%) | 70 (36.5%) | 108 (56.3%) | 14 (7.3%) |
| *myf5* mRNA + *foxd3*-MO1 | 600 pg + 8 ng | 214/396 (54%) | 88 (41.0%) | 143 (56.1%) | 6 (2.8%) |
| *dsRed* mRNA + *foxd3*-MO1 | 100 pg + 8 ng | 43/54 (79.6%) | 17 (39.5%) | 23 (53.5%) | 3 (7.0%) |
| *foxd3* mRNA + *pax3*-MO1 | 25 pg + 6 ng | 78/124 (62.9%) | 33 (42.3%) | 45 (57.7%) | 0 (0%) |

Fertilized eggs were injected at the 1-cell stage, and then observed at the 13- to 16-somite stage. Embryos with abnormal phenotypes were categorized as having mild defects, such as raised tail and reduced head size, and severe defects, such as retarded development. Results are from three independent experiments. *dsRed* mRNA: served as a negative control.

divided into subclasses a–d (Kaufmann and Knöchel, 1996). Foxd3 (CWH3, Hfh2, fkd6) is in class V.

*foxd3* is expressed in the presumptive neural crest region in both chick and mouse embryos and plays a role in neural crest differentiation in multiple systems (Freyaldenhoven et al., 1997; Hromas et al., 1999; Kos et al., 2001). Overexpression of *foxd3* in a line of myeloid cells prevents them from maturing into granulocytes (Xu et al., 1998). Ectopic expression of *foxd3* in the neural tube of chicks changes the fate of cells into neural crest-like cells and can interfere with subsequent differentiation (Dottori et al., 2001). In addition to the somatic mesoderm, zebrafish *foxd3* is transcribed in the somitic mesoderm, paraxial mesoderm, and tail bud (Odenthal and Nüsslein-Volhard, 1998; Fig. 4). Whether *foxd3* is involved in myogenesis is unknown. Previously, we demonstrated that a *cis*-element (−82/−62) of zebrafish *myf5* drives somite-specific expression and represses nonspecific expression during the early development of zebrafish embryos (Chen et al., 2003). In this study, we discovered that the winged helix transcription factor *foxd3* interacts specifically with the *myf5* −82/−62 cassette (Fig. 2). The dual-luciferase assay revealed that the expression of Foxd3 potently transactivated the *myf5* promoter (Fig. 3) and that *foxd3* plays an important role in mediating *myf5* expression during somitogenesis.

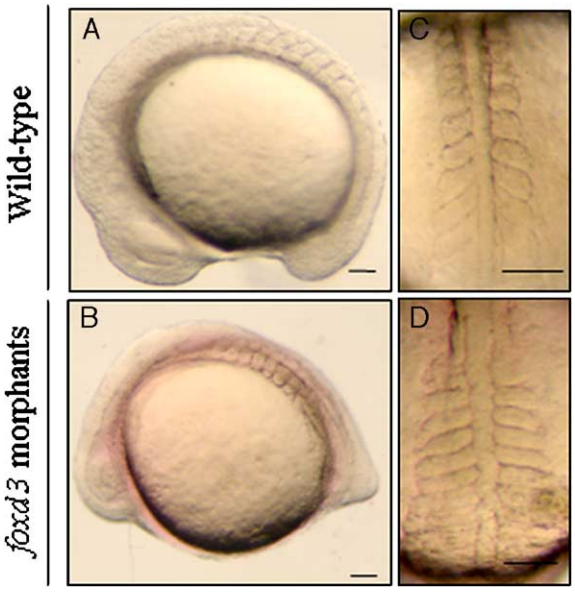


Fig. 5. The effect of inhibiting Foxd3 protein translation on somitogenesis in zebrafish embryos. Lateral and dorsal views of wild-type (upper panels) and *foxd3*-MO1-injected (lower panels) 12- to 14-somite stage embryos. Embryos that were injected with 10 ng of *foxd3*-MO1 displayed an abnormal phenotype, including an abnormal tail bud, a reduced head (A vs. B), and wider somites with an irregular somite boundary (C vs. D). Scale bars: 100 μm.

### *Foxd3 is necessary for maintaining myf5 expression in somites*

Many regulatory modules are thought to be responsible for directing the spatiotemporal expression of *myf5*. Transplantation and knockout studies in mice indicate the somites are induced by factors secreted from a variety of adjacent tissues, such as Shh (Fan and Tessier-Lavigne, 1994), Wnts (Münsterberg et al., 1995; Stern et al., 1995), Pax3 (Maroto et al., 1997; Tajbakhsh et al., 1997), and BMP (Pourquié et al., 1996; Dietrich et al., 1998). These environmental signals affect the initiation and continued expression of *myf5* in the somites. Here, we find that Foxd3, another regulatory module, has a novel function in *myf5* expression due to the finding that down-regulation of *foxd3* suppresses *myf5* expression in the somites.

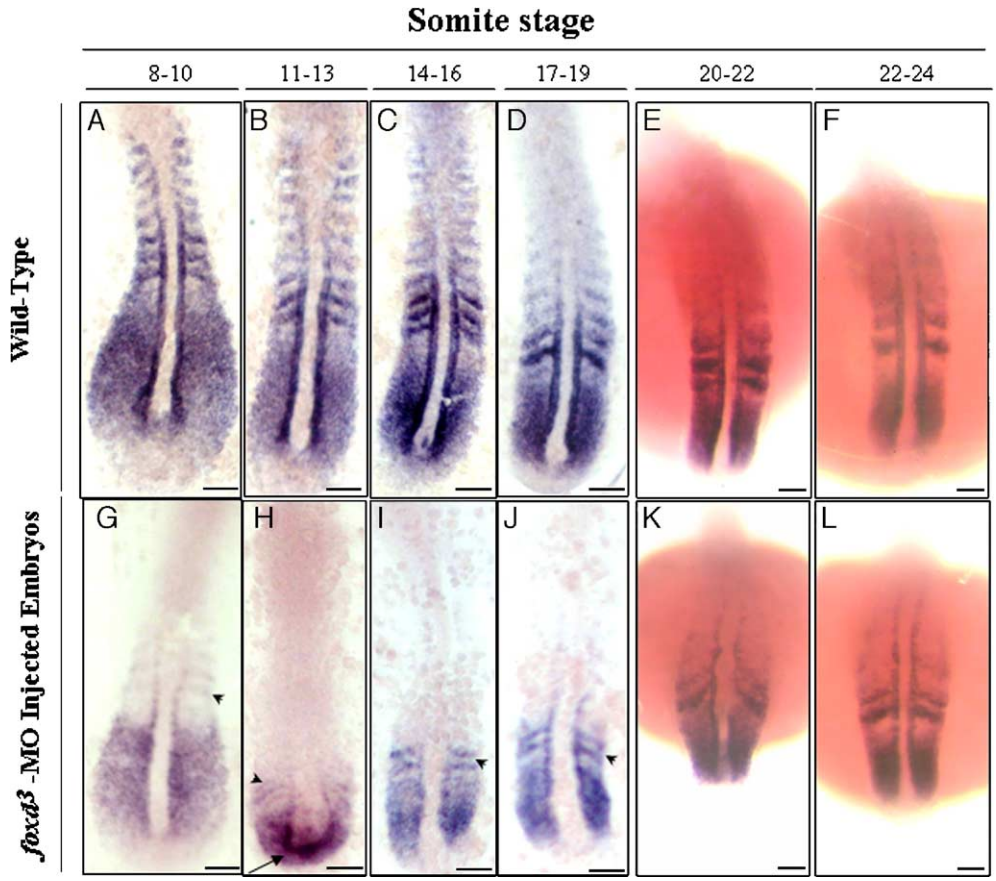


Fig. 6. Whole-mount in situ hybridizations showing gene expression in wild-type (A–F) and the *foxd3*-MO1-injected embryos (G–L) at different somite stages. In embryos with 8 to 19 somites, *myf5* expression in the somites and adaxial cells of *foxd3*-MO1-injected (10 ng) embryos was much lower than in wild-type embryos. Weak *myf5* signals appeared in somites 0 and −1 (arrowheads) and in presomitic mesoderm. Ectopic expression of *myf5* was observed in the tail bud (arrow in H). By the 20- to 24-somite stage, *myf5* expression patterns in *foxd3*-MO1-injected and wild-type embryos were similar (E, F vs. K, L). Scale bars: 100 μm.

*myf5* expression decreases dramatically in the somites and adaxial cells in the Foxd3 knockdown embryos (Figs. 6C, I). Addition of *myf5* mRNA effectively rescues the expression of both *myogenin* and α-*actin* (Fig. 7) in the somites of *foxd3* morphants, indicating that *foxd3* modulates *myf5* expression specifically. However, *myf5* expression remains unchanged in the PSM of Foxd3 knockdown embryos. The endogenous *foxd3* is not expressed in the PSM (Odenthal and Nüsslein-Volhard, 1998; Fig. 4). Therefore, we propose that *foxd3* functions in newly formed somites but not in the PSM.

The expression of zebrafish *myf5* is stage-specific and is restricted, particularly in the posterior part of each somite (Chen et al., 2001; Coutelle et al., 2001). Very little is known about the regulators that are involved in this delicate expression of *myf*5. In this report, we demonstrate clearly that Foxd3 is a *trans*-acting factor that binds directly at the upstream *cis*-elements of zebrafish *myf5* gene. Knockdown of Foxd3 level leads to a reduction of *myf5* transcripts in the newly formed somites but not in the PSM (Fig. 6). Thus, we propose that Foxd3 functions to maintain the continued expression of *myf5* in the somites but does not function to initiate *myf5* expression in the PSM. Moreover, we find that *myf5* and *foxd3* transcripts are co-localized in the posterior part of newly formed somites. Misexpression of *foxd3* leads to the ectopic expression of *myf5* but not *myod* (data not show). These results indicate that *foxd3* may function to restrict *myf5* expression in the posterior part of somites. In addition, *myod* was expressed normally in the posterior part of the somites in the *foxd3* morphants, suggesting that the mechanism of restricting expression of *myf5* is independent of *myod*.

Compared with the expression pattern of *myf5*, *foxd3* transcripts reached a relatively high level at the 9- to 18-somite stage, then *foxd*3 was down-regulated rapidly after 24 hpf (Odenthal and Nüsslein-Volhard, 1998; data not shown). Similarly, *myf5* transcripts increased substantially until the 16- to 18-somite stage and then declined gradually to an undetectable level by 26 hpf (Chen et al., 2001). In this report, we find that *myf5* expression patterns in the wild-type embryos and in the *foxd3* morphants are similar after the 20- to 22-somite stage, although the expression level of *foxd3* in the somites was still strong at these stages. However, zebrafish *myf5* transcripts in the somites became weaker and weaker after the 14- to 16-somite stage, and the transcripts were present only in the PSM close to the tail bud by 24 hpf (Chen et al., 2001). Taken together, we propose that the *foxd3* modulation on *myf5* expression is stage-dependent. Foxd3 is required for *myf5* activation in the somites between the 7- to 18-somite stage, suggesting different factors and mechanisms are involved in *myf5* down-regulation or perturbed Foxd3 functions in *myf5* activation after the 17-somite stage.

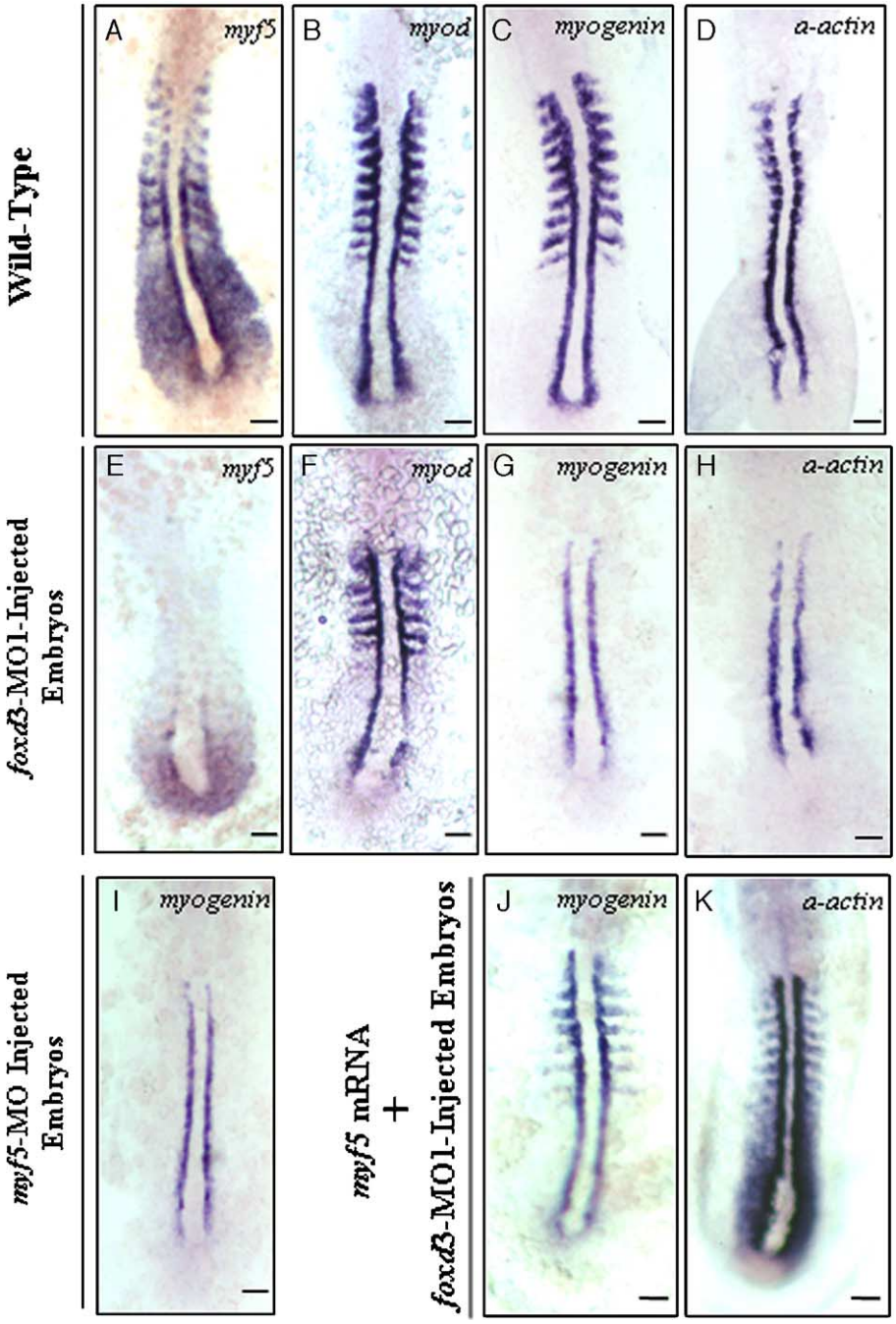


Fig. 7. Effect of inhibiting Foxd3 protein synthesis on *myf5*, *myod*, *myogenin,* and α-*actin* expression in embryos with 10–12 somites. In *foxd3*-MO1-injected (10 ng) embryos, *myf5* expression in the somites, adaxial cells, and presomitic mesoderm was reduced dramatically (A vs. E) but *myod* expression was unchanged (B vs. F). In *foxd3*-MO1-injected embryos, the expression of *myogenin* (C vs. G) and α-*actin* (D vs. H) was abolished in the somites, except in adaxial cells. Embryos injected with 4 ng of *myf5*-MO exhibited reduced *myogenin* expression in the somites, a finding similar to the defective phenotype of *foxd3* morphants (I vs. G). Co-injection of 600 ng/μl *myf5*-capped mRNA rescued expression of *myogenin* (J) and α-*actin* (K) in *foxd3*-MO1-injected embryos. Scale bars: 100 μm.

We also found that *foxd3* morphants express *myf5* ectopically in the tail bud (Fig. 6H). However, cells located in the tail bud do not express *myf5* or *myod*. Endogenous *foxd3* also was expressed in the tail bud. There are two explanations for this finding: first, we propose that *foxd3* mediates *myf5* expression in the somites differently than in the tail bud. The function of *foxd3* may be similar to the Wnt signal, which has different effects on the cranial paraxial mesoderm and on the trunk (Tzahor et al., 2003). Second, the effect may be due to a convergence-extension defect during gastrulation. Zebrafish mutants, such as *spadetail*, have a severe defect in convergence-extension of the trunk paraxial mesoderm. They lose trunk somites, resulting in paraxial mesoderm cells accumulating in the tail (Kimmel et al., 1989). These hypotheses merit further investigation.

In *foxd3* morphants, the morphological changes we find by 24 hpf are that somites become wider, with an irregular somite boundary (Figs. 5C, D). But these embryos are able to twitch as

Table 2
Rescue experiment: *myogenin* and α-*actin* expressions in the zebrafish embryos co-injected with *myf5* mRNA and *foxd3*-MO1

| Co-injection of 8 ng *foxd3*-MO1 and different concentrations of *myf5* mRNA | *myogenin* | | | | α-*actin* | | | |
|---|---|---|---|---|---|---|---|---|
| | Experimental embryos | No expression[a] | Partial expression[b] | Wild-type embryos | Experimental embryos | No expression[a] | Partial expression[b] | Wild-type embryos |
| 0 pg | 67 | 54 (81%) | 5 (7%) | 8 (12%) | 72 | 49 (68%) | 13 (32%) | 10 (14%) |
| 300 pg | 235 | 117 (50%) | 43 (18%) | 75 (32%) | 164 | 44 (27%) | 72 (44%) | 48 (29%) |
| 600 pg | 186 | 15 (8%) | 95 (51%) | 76 (41%) | 129 | 19 (15%) | 68 (53%) | 42 (32%) |

Embryos were co-injected with different concretion of *myf5* mRNA and 8 ng *foxd3*-MO1, then fixed at 16-hpf and examined by whole mount in situ hybridization for *myogenin* and α-*actin*.
[a] The number of embryos that did not exhibit expression in the somites.
[b] The number of embryos that exhibited weak expression in the somites.

normal as wild-type embryos. We also observe that the morphology of *foxd3* morphants remains unchanged during 3 to 5 days post-fertilization. Moreover, only embryos that received both *myf5*- and *myod*-MO lost somites (data not shown). Nevertheless, embryos that received *foxd3*-, *myf5*-, or *myod*-MO alone still were able to develop somites normally. Taken together, these findings may be because *myf5* and *myod* have complementary functions during somitogenesis. The function of zebrafish Myf5 is redundant during somitogenesis. However, whether Myf5 and Myod still play complementary roles in the muscle system other than somite, such as craniofacial muscle development, is worthwhile to study.

In the caudal region, paraxial mesoderm is produced by gastrulation in the primitive streak or tail bud. The *foxd3*-MO-injected embryos displayed abnormal heads, defective tails, and wider somites (Figs. 5). Moreover, *myf5* mRNA did not rescue the morphological defects induced by *foxd3*-MO1 (Table 1). We speculate this abnormal phenotype may be due to a convergence-extension defect during gastrulation, but may be not related during somitogenesis. In zebrafish, Odenthal and Nüsslein-Volhard (1998) demonstrated that there is a strong expression of *foxd3* in the involuting dorsal mesoderm. Mutation in zebrafish *trilobite* (*tri*) or *knypek* (*kny*) gene affects the convergence-extension movements. Somites in the *tri*, *kny*, or *kny;tri* mutant appear substantially wider in their mediolateral dimension (Solnica-Krezel et al., 1996; Marlow et al., 1998; Sepich et al., 2000; Henry et al., 2000). In mouse, Foxd3$^{-/-}$ embryos are dead after implantation at approximately 6.5 days post coitum, with a loss of epiblast cells, expansion of proximal extraembryonic tissues, and a distal, mislocalized anterior organizing center, suggesting that Foxd3 is required for maintaining embryonic cells of the early mouse embryo (Hanna et al., 2002). Taken together, it is highly possible that zebrafish Foxd3 may function during gastrulation. Loss of Foxd3 function causes abnormal heads, abnormal tails, and wider somites, evident as the defective phenotype displayed by *foxd3* morphants.

### *Regulation of myf5 by pax3 is mediated by foxd3*

Pax3 belongs to the family of paired-box-containing transcription factors. It is expressed in developing somites, the dorsal spinal cord, mesencephalon, and neural crest derivatives. Heterozygous *Splotch* mice are characterized by pigmentation defects due to a disorder in neural crest formation. Furthermore, homozygous embryos exhibit neural defects, including spina bifida and exencephaly (Tremblay and Gruss, 1994). All neural crest derivatives caudal to the boundary of the hindbrain and spinal cord are lost. In addition, *foxd3* is not expressed in the caudal region of *Splotch* mutants, where dorsal root ganglia and sympathetic ganglia are missing. Thus, in dorsal neural tube progenitors, *foxd3* is genetically downstream of *pax3* (Dottori et al., 2001). Ectopic expression of *pax3* throughout the neural tube alters the dorsal–ventral characteristics of the neural tube, represses floor plate formation, and decreases motor neuron differentiation in transgenic mice embryos (Tremblay et al., 1996). Forced expression of *pax3* can activate expression of both *myod* and *myf5* in paraxial mesoderm cultures and in neural tube explants. In addition, genetic and in vitro analysis determined that *pax3* regulation of mouse *myf5* is indirect (Maroto et al., 1997; Tajbakhsh et al., 1997; Roth et al., 2003).

*pax3* plays a distinct role in the development of myogenic precursors and is thought to function upstream of *myod* (Marcelle et al., 1995; Maroto et al., 1997; Tajbakhsh et al., 1997). The *Splotch* mutant lacks limb musculature (Franz et al., 1993; Bober et al., 1994), demonstrating that *pax3* is necessary for the migration of muscle precursor cells (Bober et al., 1994; Goulding et al., 1994; Marcelle et al., 1995). *myod* is not activated in the *Splotch/myf5* double null mutant, suggesting that *myod* acts genetically downstream of *pax3* and *myf5* in the establishment of skeletal muscle in the body (Tajbakhsh et al., 1997). Relaix et al. (2003) showed that *pax3* cannot directly activate the distal *myod* enhancer, indicating that *pax3* activates *myod* indirectly. Thus, whether Pax3 acts directly on *myod* in mammals remains unclear. In zebrafish, the expression of *pax3* is observed first in somites of embryos at the 6- to 8-somite stage. Transcripts are detected in most of the somites until the 14- to 16-somite stage; subsequently, expression is reduced (Seo et al., 1998). In this report, embryos that received *pax3*-MOs display severe convergence/extension phenotypes. This consequence may be because *pax3* is detected initially at the neural plate stage (Seo et al., 1998) and functions during gastrulation. Both *pax3* and *foxd3* morphants display defective convergence/extension phenotypes, and *foxd3* expression is down-regulated greatly in *pax3*-MO1-injected zebrafish embryos, suggesting that *pax3* functions upstream of *foxd3*. However, the stripe pattern of *myf5* can be rescued by *foxd3*

mRNA in *pax3* morphants (Fig. 8), but the convergence/extension phenotype cannot (Table 1). Actually, the molecular mechanism about *pax3* and *foxd3* involved in gastrulation are still unclear at the present study. Taken together, we speculate that *foxd3* may be one of the downstream target genes of *pax3* during gastrulation. Over-expression of *foxd3* in *pax3* morphants could not rescue all the functions that *pax3* plays. Besides, it is also reasonable to speculate that Pax3 and Foxd3 seems to be acting in independent ways during gastrulation.

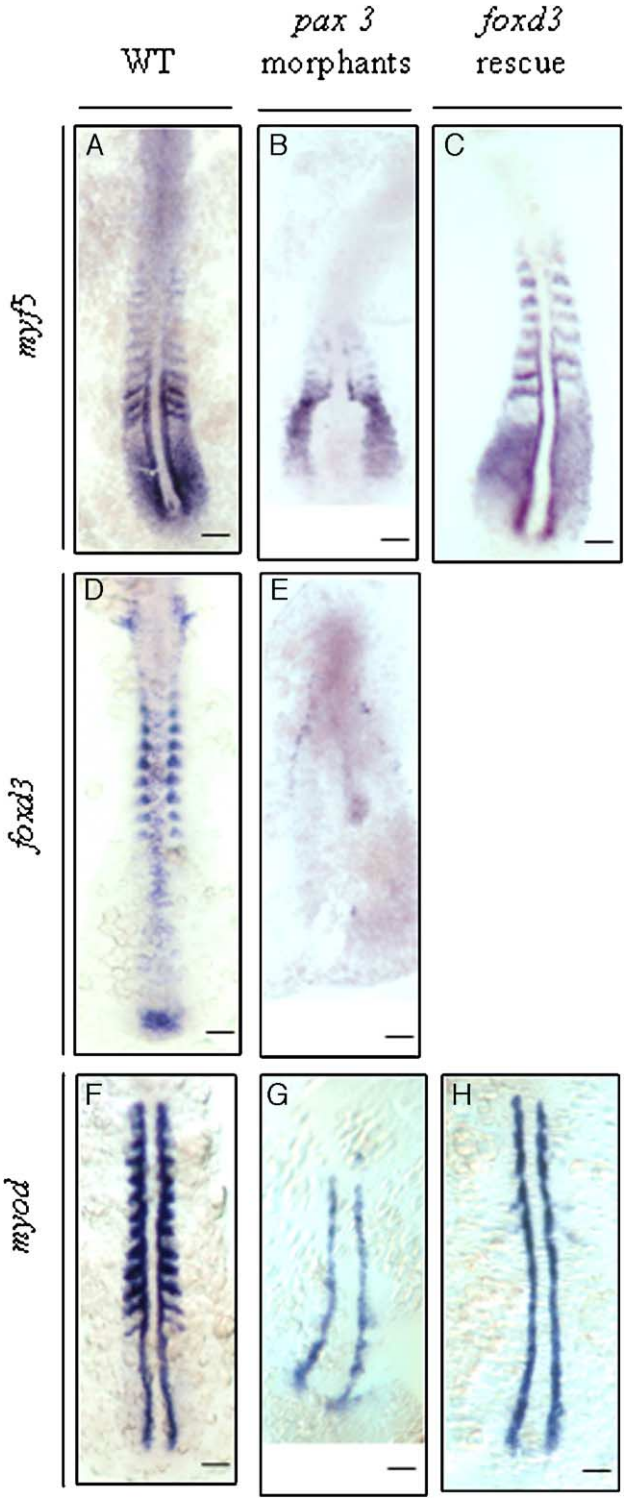


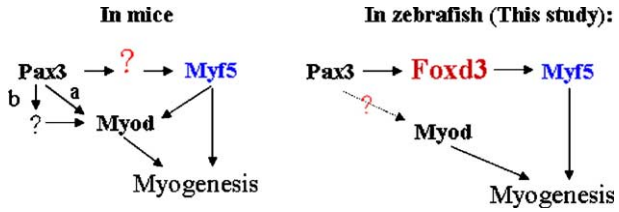


Fig. 9. Models of the *myf5* regulation network during somitogenesis in mice and zebrafish. (a) *myod* functions downstream of *pax3* (Tajbakhsh et al., 1997). (b) *pax3* activates *myod* indirectly (Relaix et al., 2003).

In *pax3* morphants, *myf5* expression is restricted to the PSM, as is the case in *foxd3* morphants. In addition, the *pax3* (Seo et al., 1998) and *foxd3* (Fig. 4) transcripts are not detectable in the PSM. Over-expression of *foxd3* mRNA in *pax3* morphants rescues the stripe patterns of *myf5* in the somites, indicating that these factors are permissive for the expression of the target genes, but not instructive. Taken together, these findings suggest that *myf5* down-regulation occurs in *pax3* morphants, because *foxd3* is not expressed. Pax3 and Foxd3 function to maintain *myf5* expression in the newly formed somites. Moreover, our analysis of zebrafish *foxd3* and *pax3* morphants demonstrated that *foxd3* specifically regulates expression of *myf5* but not *myod* (Figs. 7, 8). These data suggest that Pax3 may activate the expression of *myf5* and *myod* through a different regulatory mechanism. Therefore, we propose a model in which the signaling cascade involved in muscle development begins with *pax3* inducing *foxd3* expression, which then induces *myf5* expression (Fig. 9).

### *Delicate network of myf5 regulation during embryogenesis*

The function of cassette −82/−62 is to recruit a *trans*-factor to drive somite-specific expression. Several studies have found that a transcription factor interacts with a ubiquitous factor to drive tissue-specific expression. In neuron-specific expression, a neuron-restricted transcription factor, MASH1, interacts with CBF to drive tissue-specific expression (Mandolesi et al., 2002). Cardiac-specific expression is directed by the interaction of a heart-specific factor, myocardin, with a ubiquitous serum response factor bound to a CArG box (Wang et al., 2001). We found that the *trans*-factor Foxd3 binds to the −82/−62 *cis*-element and has a novel function during myogenesis. This function is totally distinct from previously known

Fig. 8. The effect of inhibiting Pax3 protein synthesis on the expression of *foxd3*, *myf5*, and *myod* in the zebrafish embryos at 5 to 8 somites. Probes were used to detect *myf5* (A, B, C), *foxd3* (D, E), and *myod* (F, G, H) in the wild-type embryos (A, D, F), the *pax3*-MO1-injected (6 ng) embryos (B, E, G), and the embryos co-injected with 6 ng of *pax3*-MO1 and 25 pg of *foxd3* mRNA (C, H). (B) In *pax3*-MO1-injected embryos, *myf5* expression was restricted in the presomitic mesoderm (PSM) and weak in somites 0 and −1 and in the adaxial cells on the sides of somites 0 and −1. (E) The shape of the neural plate became abnormal in the *pax3*-MO1 morphants, and *foxd3* expression was weak in their neural fold and tail bud. (G) Meanwhile, *myod* expression was down-regulated in the somites, but it was expressed in adaxial cells. In the rescue experiment, co-injection of *foxd3* mRNA and *pax3*-MO1 restored *myf5* expression in the somites (C), whereas the *myod* expression was not rescued (H). Scale bars: 100 μm.

functions of Foxd3 in neural crest development. We hypothesize that Foxd3 interacts with different cofactors in the somites and neural crest cells. In addition, we think that the effect of Foxd3 in the tail bud is different from its effect in the somites. This difference occurs because different cofactors bind to cassette −82/−62. As a result, Foxd3 plays a unique role in regulating *myf5* expression. These hypotheses merit further investigation.

A *trans*-acting factor can function as both an activator and a repressor, depending on its binding sequence and/or its interaction with a specific cofactor. Transcription factors YY1 (Shrivastava and Calame, 1994; Shi et al., 1997) and NF-Y (Peng and Jahroudi, 2002) function in this way. Moreover, the ectopic expression of Foxd3 in the chick neural tube induces expression of migratory neural crest markers but suppresses interneuron differentiation (Dottori et al., 2001). Over-expression of Foxd3 prevents the migration of neural crest cells along the dorsolateral migratory pathway, suggesting that Foxd3 suppresses melanogenesis (Kos et al., 2001). We found that Foxd3 has opposite effects in the somites and tail bud and can function as both an activator and a repressor. Recently, we reported that a *cis*-acting element in the downstream region (+502/+835) of zebrafish *myf5* intron 1 represses *myf5* expression (Lin et al., 2004). On the basis of these results, we hypothesize that the zebrafish *myf5* −82/−62 cassette, the intron 1 +502/+835 element, Foxd3 and other unknown factors, and even a *cis*-element located in the distal upstream region form a huge complex that orchestrates the spatiotemporal expression of *myf5* during somitogenesis.

In summary, we characterized signals that modulate somitogenesis. Our results reveal that the winged helix transcription factor Foxd3 plays an important role in maintaining *myf5* expression in the newly formed somites and the adaxial cells. We propose a model of gene regulation in which *pax3* induces *foxd3* expression, which then induces the expression of *myf5*. However, because inhibition of *foxd3* translation does not completely abolish *myf5* expression in the PSM, we speculate that factors other than Foxd3 are involved in regulating *myf5* expression in the PSM.

## Acknowledgment

This work was supported by the National Science Council, Republic of China, under grant NSC 94-2313-B002-073.

## References

Bober, E., Franz, T., Arnold, H.H., Gruss, P., Tremblay, P., 1994. Pax-3 is required for the development of limb muscles: a possible role for the migration of dermomyotomal muscle progenitor cells. Development 120, 603–612.

Borycki, A.G., Brunk, B., Tajbakhsh, S., Buckingham, M., Chiang, C., Emerson Jr., C.P., 1999. Sonic hedgehog controls epaxial muscle determination through Myf5 activation. Development 126, 4053–4063.

Braun, T., Bober, E., Buschhausen-Denker, G., Kohtz, S., Grzeschik, K.H., Arnold, H.H., 1989a. Differential expression of myogenic determination genes in muscle cells: possible autoactivation by the Myf gene products. EMBO J. 8, 3617–3625.

Braun, T., Buschhausen-Denker, G., Bober, E., Tannich, E., Arnold, H.H., 1989b. A novel human muscle factor related to but distinct from MyoD1 induces myogenic conversion in 10T1/2 fibroblasts. EMBO J. 8, 701–709.

Braun, T., Bober, E., Winter, B., Rosenthal, N., Arnold, H.H., 1990. Myf-6, a new member of the human gene family of myogenic determination factors: evidence for a gene cluster on chromosome 12. EMBO J. 9, 821–831.

Buchberger, A., Nomokonova, N., Arnold, H.H., 2003. Myf5 expression in somites and limb buds of mouse embryos is controlled by two distinct distal enhancer activities. Development 130, 3297–3307.

Buckingham, M., 2001. Skeletal muscle formation in vertebrates. Curr. Opin. Genet. Dev. 11, 440–448.

Buonanno, A., Apone, L., Morasso, M.I., Beers, R., Brenner, H.R., Eftimie, R., 1992. The MyoD family of myogenic factors is regulated by electrical activity: isolation and characterization of a mouse Myf5 cDNA. Nucleic Acids Res. 20, 539–544.

Carvajal, J.J., Cox, D., Summerbell, D., Rigby, P.W., 2001. A BAC transgenic analysis of the Mrf4/Myf5 locus reveals interdigitated elements that control activation and maintenance of gene expression during muscle development. Development 128, 1857–1868.

Chen, Y.H., Lee, W.C., Cheng, C.H., Tsai, H.J., 2000. Muscle regulatory factor gene: zebrafish (*Danio rerio*) myogenin cDNA. Comp. Biochem. Physiol., Part B: Biochem. Mol. Biol. 127, 97–103.

Chen, Y.H., Lee, W.C., Liu, C.F., Tsai, H.J., 2001. Molecular structure, dynamic expression, and promoter analysis of zebrafish (*Danio rerio*) *myf-5* gene. Genesis 29, 22–35.

Chen, Y.H., Lee, H.C., Liu, C.F., Lin, C.Y., Tsai, H.J., 2003. Novel regulatory sequence −82/−62 functions as a key element to drive the somite-specificity of zebrafish *myf5*. Dev. Dyn. 228, 41–50.

Cossu, G., Borello, U., 1999. Wnt signaling and the activation of myogenesis in mammals. EMBO J. 18, 6867–6872.

Cossu, G., Tajbakhsh, S., Buckingham, M., 1996. How is myogenesis initiated in the embryo? Trends Genet. 12, 218–223.

Coutelle, O., Blagden, C.S., Hampson, R., Halai, C., Rigby, P.W., Hughes, S.M., 2001. Hedgehog signalling is required for maintenance of *myf5* and *myod* expression and timely terminal differentiation in zebrafish adaxial myogenesis. Dev. Biol. 236, 136–150.

Currie, P.D., Ingham, P.W., 1998. The generation and interpretation of positional information within the vertebrate myotome. Mech. Dev. 73, 3–21.

Davis, R.L., Weintraub, H., Lassar, A.B., 1987. Expression of a single transfected cDNA converts fibroblasts to myoblasts. Cell 51, 987–1000.

Dietrich, S., Schubert, F.R., Healy, C., Sharpe, P.T., Lumsden, A., 1998. Specification of the hypaxial musculature. Development 125, 2235–2249.

Dottori, M., Gross, M.K., Labosky, P., Goulding, M., 2001. The winged-helix transcription factor Foxd3 suppresses interneuron differentiation and promotes neural crest cell fate. Development 128, 4127–4138.

Edmondson, D.G., Olson, E.N., 1989. A gene with homology to the myc similarity region of MyoD1 is expressed during myogenesis and is sufficient to activate the muscle differentiation program. Genes Dev. 3, 628–640.

Fan, C.M., Tessier-Lavigne, M., 1994. Patterning of mammalian somites by surface ectoderm and notochord: evidence for sclerotome induction by a hedgehog homolog. Cell 79, 1175–1186.

Franz, T., Kothary, R., Surani, M.A., Halata, Z., Grim, M., 1993. The *Splotch* mutation interferes with muscle development in the limbs. Anat. Embryol. (Berl.) 187, 153–160.

Freyaldenhoven, B.S., Freyaldenhoven, M.P., Iacovoni, J.S., Vogt, P.K., 1997. Avian winged helix proteins CWH-1, CWH-2 and CWH-3 repress transcription from Qin binding sites. Cancer Res. 57, 123–129.

Goulding, M., Lumsden, A., Paquette, A.J., 1994. Regulation of Pax-3 expression in the dermomyotome and its role in muscle development. Development 120, 957–971.

Gustafsson, M.K., Pan, H., Pinney, D.F., Liu, Y., Lewandowski, A., Epstein, D.J., Emerson Jr., C.P., 2002. Myf5 is a direct target of long-range Shh signaling and Gli regulation for muscle specification. Genes Dev. 16, 114–126.

Hadchouel, J., Tajbakhsh, S., Primig, M., Chang, T.H., Daubas, P., Rocancourt, D., Buckingham, M., 2000. Modular long-range regulation of Myf5 reveals

unexpected heterogeneity between skeletal muscles in the mouse embryo. Development 127, 4455–4467.
Hanna, L.A., Foreman, R.K., Tarasenko, I.A., Kessler, D.S., Labosky, P.A., 2002. Requirement for Foxd3 in maintaining pluripotent cells of the early mouse embryo. Genes Dev. 16, 2650–2661.
Henry, C.A., Hall, L.A., Burr Hille, M., Solnica-Krezel, L., Cooper, M.S., 2000. Somites in zebrafish doubly mutant for *knypek* and *trilobite* form without internal mesenchymal cells or compaction. Curr. Biol. 7, 1063–1066.
Hirsinger, E., Duprez, D., Jouve, C., Malapert, P., Cooke, J., Pourquié, O., 1997. Noggin acts downstream of Wnt and Sonic Hedgehog to antagonize BMP4 in avian somite patterning. Development 124, 4605–4614.
Hopwood, N.D., Pluck, A., Gurdon, J.B., 1991. *Xenopus* Myf5 marks early muscle cells and can activate muscle genes ectopically in early embryos. Development 111, 551–560.
Hromas, R., Ye, H., Spinella, M., Dmitrovsky, E., Xu, D., Costa, R.H., 1999. Genesis, a Winged Helix transcriptional repressor, has embryonic expression limited to the neural crest, and stimulates proliferation in vitro in a neural development model. Cell Tissue Res. 297, 371–382.
Ikeya, M., Takada, S., 1998. Wnt signaling from the dorsal neural tube is required for the formation of the medial dermomyotome. Development 125, 4969–4976.
Jowett, T., 2001. Double in situ hybridization techniques in zebrafish. Methods 23, 345–358.
Kaufmann, E., Knöchel, W., 1996. Five years on the wings of fork head. Mech. Dev. 57, 3–20.
Kimmel, C.B., Kane, D.A., Walker, C., Warga, R.M., Rothman, M.B., 1989. Amutation that changes cell movement and cell fate in the zebrafish embryo. Nature 337, 358–362.
Kos, R., Reedy, M.V., Johnson, R.L., Erickson, C.A., 2001. The winged-helix transcription factor FoxD3 is important for establishing the neural crest lineage and repressing melanogenesis in avian embryos. Development 128, 1467–1479.
Krause, M., Harrison, S.W., Xu, S.Q., Chen, L., Fire, A., 1994. Elements regulating cell- and stage-specific expression of the *C. elegans* MyoD family homolog *hlh-1*. Dev. Biol. 166, 133–148.
Lai, E., Prezioso, V.R., Smith, E., Litvin, O., Costa, R.H., Damell Jr., J.E., 1990. HNF-3A, a hepatocyte-enriched transcription factor of novel structure is regulated transcriptionally. Genes Dev. 4, 1427–1436.
Lai, E., Prezioso, V.R., Tao, W.F., Chen, W.S., Damell Jr., J.E., 1991. Hepatocyte nuclear factor 3 alpha belongs to a gene family in mammals that is homologous to the *Drosophila* homeotic gene fork head. Genes Dev. 5, 416–427.
Lai, E., Clark, K.L., Burley, S.K., Darnell Jr., J.E., 1993. Hepatocyte nuclear factor 3/fork head or "winged helix" proteins: a family of transcription factors of diverse biologic function. Proc. Natl. Acad. Sci. U. S. A. 90, 10421–10423.
Lin, G.F., Geng, X., Chen, Y., Qu, B., Wang, F., Hu, R., Ding, X., 2003. T-box binding site mediates the dorsal activation of myf-5 in *Xenopus* gastrula embryos. Dev. Dyn. 226, 51–58.
Lin, C.Y., Chen, Y.H., Lee, H.C., Tsai, H.J., 2004. Novel *cis*-element in intron 1 represses somite expression of zebrafish *myf5*. Gene 334, 63–72.
Mandolesi, G., Gargano, S., Pennuto, M., Illi, B., Molfetta, R., Soucek, L., Mosca, L., Levi, A., Jucker, R., Nasi, S., 2002. NGF-dependent and tissue-specific transcription of vgf is regulated by a CREB-p300 and bHLH factor interaction. FEBS Lett. 510, 50–56.
Marcelle, C., Wolf, J., Bronner-Fraser, M., 1995. The in vivo expression of the FGF receptor FREK mRNA in avian myoblasts suggests a role in muscle growth and differentiation. Dev. Biol. 172, 100–114.
Marcelle, C., Stark, M.R., Bronner-Fraser, M., 1997. Coordinate actions of BMPs, Wnts, Shh and noggin mediate patterning of the dorsal somite. Development 124, 3955–3963.
Marlow, F., Zwartkruis, F., Malicki, J., Neuhauss, S.C., Abbas, L., Weaver, M., Driever, W., Solnica-Krezel, L., 1998. Functional interactions of genes mediating convergent extension, *knypek* and *trilobite*, during the partitioning of the eye primordium in zebrafish. Dev. Biol. 203, 382–399.
Maroto, M., Reshef, R., Münsterberg, A.E., Koester, S., Goulding, M., Lassar, A.B., 1997. Ectopic Pax-3 activates MyoD and Myf5 expression in embryonic mesoderm and neural tissue. Cell 89, 139–148.
Mei, W., Yang, J., Tao, Q., Geng, X., Rupp, R.A., Ding, X., 2001. An interferon regulatory factor-like binding element restricts *Xmyf-5* expression in the posterior somites during *Xenopus* myogenesis. FEBS Lett. 505, 47–52.
Michelson, A.M., Abmayr, S.M., Bate, M., Arias, A.M., Maniatis, T., 1990. Expression of a MyoD family member prefigures muscle pattern in *Drosophila* embryos. Genes Dev. 4, 2086–2097.
Miner, J.H., Wold, B., 1990. Herculin, a fourth member of the MyoD family of myogenic regulatory genes. Proc. Natl. Acad. Sci. U. S. A. 87, 1089–1093.
Münsterberg, A.E., Kitajewski, J., Bumcrot, D.A., McMahon, A.P., Lassar, A.B., 1995. Combinatorial signaling by Sonic hedgehog and Wnt family members induces myogenic bHLH gene expression in the somite. Genes Dev. 9, 2911–2922.
Odenthal, J., Nüsslein-Volhard, C., 1998. fork head domain genes in zebrafish. Dev. Genes Evol. 208, 245–258.
Peng, Y., Jahroudi, N., 2002. The NFY transcription factor inhibits von Willebrand factor promoter activation in non-endothelial cells through recruitment of histone deacetylases. Blood 99, 2408–2417.
Pourquié, O., Fan, C.M., Coltey, M., Hirsinger, E., Watanabe, Y., Breant, C., Francis-West, P., Brickell, P., Tessier-Lavigne, M., Le Douarin, N.M., 1996. Lateral and axial signals involved in avian somite patterning: a role for BMP4. Cell 84, 461–471.
Relaix, F., Polimeni, M., Rocancourt, D., Ponzetto, C., Schafer, B.W., Buckingham, M., 2003. The transcriptional activator PAX3-FKHR rescues the defects of Pax3 mutant mice but induces a myogenic gain-of-function phenotype with ligand-independent activation of Met signaling in vivo. Genes Dev. 17, 2950–2965.
Reshef, R., Maroto, M., Lassar, A.B., 1998. Regulation of dorsal somitic cell fates: BMPs and Noggin control the timing and pattern of myogenic regulator expression. Genes Dev. 12, 290–303.
Rhodes, S.J., Konieczny, S.F., 1989. Identification of MRF4: a new member of the muscle regulatory factor gene family. Genes Dev. 3, 2050–2061.
Roth, J.F., Shikama, N., Henzen, C., Desbaillets, I., Lutz, W., Marino, S., Wittwer, J., Schorle, H., Gassmann, M., Eckner, R., 2003. Differential role of p300 and CBP acetyltransferase during myogenesis: p300 acts upstream of MyoD and Myf5. EMBO J. 22, 5186–5196.
Saitoh, O., Fujisawa-Sehara, A., Nabeshima, Y., Periasamy, M., 1993. Expression of myogenic factors in denervated chicken breast muscle: isolation of the chicken Myf5 gene. Nucleic Acids Res. 21, 2503–2509.
Seo, H.C., Saetre, B.O., Havik, B., Ellingsen, S., Fjose, A., 1998. The zebrafish Pax3 and Pax7 homologues are highly conserved, encode multiple isoforms and show dynamic segment-like expression in the developing brain. Mech. Dev. 70, 49–63.
Sepich, D.S., Myers, D.C., Short, R., Topczewski, J., Marlow, F., Solnica-Krezel, L., 2000. Role of the zebrafish trilobite locus in gastrulation movements of convergence and extension. Genesis 27, 159–173.
Shi, Y., Lee, J.S., Galvin, K.M., 1997. Everything you have ever wanted to know about Yin Yang 1…. Biochim. Biophys. Acta 1332, F49–F66.
Shrivastava, A., Calame, K., 1994. An analysis of genes regulated by the multi-functional transcriptional regulator Yin Yang-1. Nucleic Acids Res. 22, 5151–5155.
Solnica-Krezel, L., Stemple, D.L., Mountcastle-Shah, E., Rangini, Z., Neuhauss, S.C., Malicki, J., Schier, A.F., Stainier, D.Y., Zwartkruis, F., Abdelilah, S., Driever, W., 1996. Mutations affecting cell fates and cellular rearrangements during gastrulation in zebrafish. Development 123, 67–80.
Stern, H.M., Brown, A.M., Hauschka, S.D., 1995. Myogenesis in paraxial mesoderm: preferential induction by dorsal neural tube and by cells expressing Wnt-1. Development 121, 3675–3686.
Summerbell, D., Ashby, P.R., Coutelle, O., Cox, D., Yee, S., Rigby, P.W., 2000. The expression of Myf5 in the developing mouse embryo is controlled by discrete and dispersed enhancers specific for particular populations of skeletal muscle precursors. Development 127, 3745–3757.
Tajbakhsh, S., 2003. Stem cells to tissue: molecular, cellular and anatomical heterogeneity in skeletal muscle. Curr. Opin. Genet. Dev. 13, 413–422.
Tajbakhsh, S., Rocancourt, D., Cossu, G., Buckingham, M., 1997. Redefining the genetic hierarchies controlling skeletal myogenesis: Pax-3 and Myf5 act upstream of MyoD. Cell 89, 127–138.
Tajbakhsh, S., Borello, U., Vivarelli, E., Kelly, R., Papkoff, J., Duprez, D., Buckingham, M., Cossu, G., 1998. Differential activation of Myf5 and

MyoD by different Wnts in explants of mouse paraxial mesoderm and the later activation of myogenesis in the absence of Myf5. Development 125, 4155–4162.

Tremblay, P., Gruss, P., 1994. Pax: genes for mice and men. Pharmacol. Ther. 61, 205–226.

Tremblay, P., Pituello, F., Gruss, P., 1996. Inhibition of floor plate differentiation by Pax3: evidence from ectopic expression in transgenic mice. Development 122, 2555–2567.

Tzahor, E., Kempf, H., Mootoosamy, R.C., Poon, A.C., Abzhanov, A., Tabin, C.J., Dietrich, S., Lassar, A.B., 2003. Antagonists of Wnt and BMP signaling promote the formation of vertebrate head muscle. Genes Dev. 17, 3087–3099.

Wang, D., Chang, P.S., Wang, Z., Sutherland, L., Richardson, J.A., Small, E., Krieg, P.A., Olson, E.N., 2001. Activation of cardiac gene expression by myocardin, a transcriptional cofactor for serum response factor. Cell 105, 851–862.

Weigel, D., Jäckle, H., 1990. The fork head domain: a novel DNA binding motif of eukaryotic transcription factors? Cell 63, 455–456.

Weigel, D., Jurgens, G., Kuttner, F., Seifert, E., Jackle, H., 1989. The homeotic gene fork head encodes a nuclear protein and is expressed in the terminal regions of the *Drosophila* embryo. Cell 57, 645–658.

Wright, W.E., Sassoon, D.A., Lin, V.K., 1989. Myogenin, a factor regulating myogenesis, has a domain homologous to MyoD. Cell 56, 607–617.

Xu, D., Yoder, M., Sutton, J., Hromas, R., 1998. Forced expression of Genesis, a winged helix transcriptional repressor isolated from embryonic stem cells, blocks granulocytic differentiation of 32D myeloid cells. Leukemia 12, 207–212.

Yamaguchi, T.P., 1997. New insights into segmentation and patterning during vertebrate somitogenesis. Curr. Opin. Genet. Dev. 7, 513–518.

Yang, J., Mei, W., Otto, A., Xiao, L., Tao, Q., Geng, X., Rupp, R.A., Ding, X., 2002. Repression through a distal TCF-3 binding site restricts *Xenopus* myf-5 expression in gastrula mesoderm. Mech. Dev. 115, 79–89.